



Semnan University



The Effect of External Skin on Buckling Strength of Composite Lattice Cylinders Based on Numerical and Experimental Analysis

M.R. Zamani *, S.M.R. Khalili

Department of Mechanical Engineering, K.N. Toosi University of Technology, Tehran, Iran

PAPER INFO

Paper history:

Received: 2016-02-27

Revised: 2016-07-08

Accepted: 2016-08-04

Keywords:

Lattice structures

Buckling

FEM

Stiffened composite cylindrically shell

ABSTRACT

Currently, lattice composite structures have many applications in aerospace industries. The present research analyzed the effect of an external skin consisting of a lattice's cylindrical shell on the buckling strength of composite materials, both numerically and experimentally. Two classes of specimens, with and without external skins, were fabricated using the filament winding process. To find the buckling strength of the fabricated samples, tests were carried out. For validation of the experimental results, the finite element method was used to test the shells under the same testing conditions. The results of the experimental and numerical tests showed good agreement with one another, revealing that the lattice cylindrical shell specimen with the outer skin had a much higher buckling strength than the one without the outer skin ($\approx 50\%$). The added weight of the outer skin was negligible compared to the overall weight of the lattice cylindrical shell, and the external skin had a tremendous positive effect on the buckling strength to weight ratio of the lattice composite structures.

© 2016 Published by Semnan University Press. All rights reserved.

1. Introduction

In the case of high compressive loads, lattice cylindrical shells are very reliable due to their high stiffness and strength. In addition, when these structures are made by composite materials, they become more efficient than solely metal structures. Buckling can occur in different forms, such as global and local deflections, and buckling can lead to the collapse of the structure. Thus, avoiding buckling failure is an essential criterion in the design of structural components.

Kidane et al. [1] analysed the buckling of grid-stiffened composite cylinders and developed an analytical model for determination of the equivalent stiffness parameters for a grid stiffened with a composite cylindrical shell. Ghasemi et al. [2] studied the effects of shell thickness, angle of fibers in the shell, and the direction of stiffeners under the buckling load. First-order shear deformation theory, based on the Ritz method, was used to calculate the critical buckling load of those structures. Khalili et al. [3] studied the transient dynamic response of initially stressed composite circular cylindrical shells under a radial impulse load. The effects of fiber orientation, axial load,

internal pressure, and geometrical parameters on the time response of the shell were investigated. In addition, Arashmehr et al. [4] analysed both the numerical and the experimental stress of stiffened cylindrical composite shells under a transverse end load. In addition, a stiffened composite cylindrical shell with a clamped-free boundary condition under a transverse end load was studied both experimentally and numerically. Ghasemi et al. [5] studied the buckling of a composite-stiffened conical shell grid under axial loading, and they found that a structure with ribs of 30° and a shell winding angle between 70° - 80° provided a good case for its modified design. Vasiliev et al. [6] reviewed the recent Russian developments and applications of anisogrid composite lattice structures, where information about fabrication processes, design and analysis methods, mechanical properties of the basic structural elements, and application of the anisogrid composite design concept to aerospace structures were provided. Bisagni and Cardisco [7] studied the effects of post buckling and collapse experiments on stiffened composite cylindrical shells subjected to axial loading and torque. The

* Corresponding author, Tel.: +98-021-22987191; Fax: +98-021-22936578

E-mail address: a_mrzamani@mut.ac.ir

test results showed the strength capacity of these structures to work even in the post-buckling range. Buragohain and Velmurugan [8] investigated buckling analysis of composite hexagonal lattice cylindrical shells using a smeared stiffener model. Additionally, variations of material properties of rib unidirectional composites from those of the normal unidirectional composites were accounted for in the energy formulations. Rahimi et al. [9] investigated the effects of a stiffener profile on the buckling strength in composite isogrid-stiffened shells under axial loading. Their study showed that stiffening the shell increased the buckling load from 10% to 36%, while decreasing the buckling load to weight ratio of an unstiffened shell from 42% to 52%. An efficient finite element model for buckling analysis of grid-stiffened laminated composite plates was carried out by Huang et al. [10], in which they performed a parametric study to show the effects of skin thickness, stiffener width, and stiffener depth on the buckling capacity of grid-stiffened composite plates. Sun et al. [11] studied the buckling behaviours of shear, deformable grid-stiffened functionally-graded cylindrical shells under the combined compressive and thermal loads. The effects of geometric parameters, properties of FGMs, and temperature fields on the anti-buckling performances of grid-stiffened shells were examined under the clamped boundary condition.

This paper presents a numerical and experimental investigation of the buckling of hexagonal composite lattice cylindrical shells. The specimens were manufactured with and without shells and were fabricated with a continuous glass fiber using a specially-designed filament winding setup. In addition, finite element models were carried out using ABAQUS software, which took into consideration the exact geometric configurations of the stiffeners and the shells. Finally, the results were compared with each other and good agreement was seen between the numerical and the experimental results.

2. Finite Element Method

Figure 1 shows a section of the lattice structure with an outer skin that stiffened the helical and hoop ribs. Geometrical parameters are also shown in Figure 1. The finite element models were built for the grid-stiffened cylindrical shells with both isogrid and anisogrid types of stiffeners, using ABAQUS software for the design.

The skin and stiffeners were modelled separately. Then, the stiffeners were assembled at the interface areas and later analysed in the form of a single structure. To simulate the actual test conditions, two plates were placed at the top and bottom of the samples that had friction coefficients

of 0.6, which were appropriate for these kinds of structures.

The vertical load was transferred to the sample through the plates as in the actual test conditions. This model appears in Figure 2. The shell section was modeled by a two-ply laminate having a stacking sequence of $[+72/-72]$, with each layer having an approximate thickness of 0.3 mm. Fibers in the stiffeners were oriented along the length of the stiffeners. Shell elements with reduced integration S4R with a Mindlin formulation were used to mesh the skin and the stiffeners. The problem was solved in ABAQUS using a non-linear buckling analysis method.

3. Experimental Procedure

Two types of specimens, one with and one without a shell and having identical material properties, were fabricated using the filament winding process. The volume fraction of the fiber and resin epoxy was 70%, and this factor was configured into the filament winding. To obtain the required mechanical properties in the samples, tensile testing samples were manufactured and tested using a tensile testing machine (Gotech universal testing machine, Taiwan) according to the ASTM-D2343 standard. The tensile testing results are presented in Table 1.

Figure 3 shows the fabrication of the specimens, using the filament winding process to manufacture the samples. The ribs and the skin were made in a single step, a continuous process in which the ribs were made first and then the skin was wound immediately. Each sample contains 15 clockwise helical ribs, 15 counter-clockwise helical ribs, and 6 circumferential ribs. The geometrical cross-sectional area of the ribs consists of a quadrangle with a surface area of 20 mm². Table 2 shows the geometrical information for the specimens.

In order to test the manufactured samples, the same GOTECH tensile testing machine was used load in a displacement-controlled procedure using a rate of 0.5 mm/min. Two flat, metal, thick plates were positioned on both ends of each specimen as shown in Figure 4. The loading was increased until the structure failed.

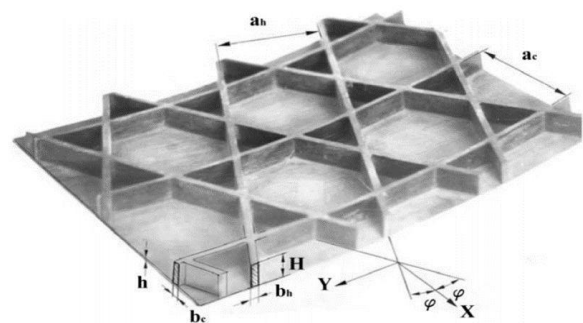


Figure 1. Unit cell of the lattice cylindrical structure [6].

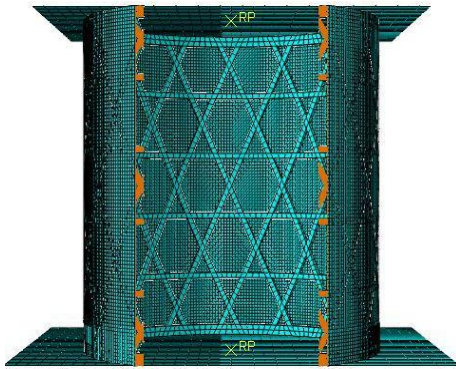


Figure 2. Finite elements' model.

Table 1. Material properties of the specimens.

Elastic Modulus				
ρ (kg/m ³)	E_{11} (GPa)	E_{22} (GPa)	ν_{12}	G_{12} (GPa)
1600	100	7.6	0.31	4.6
Ultimate Strength				
X_T (MPa)	X_C (MPa)	Y_T (MPa)	Y_C (MPa)	S (MPa)
1500	800	45	150	55
Fracture Energy				
G_{ft} (N/mm)	G_{fc} (N/mm)	G_{mt} (N/mm)	G_{mc} (N/mm)	
70	95	0.25	1	

Table 2. Geometrical information of the specimens.

Shell Information	
Shell Height (mm)	300
Outer Radius (mm)	150
Shell Thickness (mm)	0.6
Lattice Geometrical Information	
Distance between the Helical Ribs (a_h)(mm)	56.73
Distance between the Circumferential Ribs (a_c)(mm)	60
Width of the Helical Ribs (b_h)(mm)	5
Width of the Circumferential Ribs (b_c)(mm)	5
Lattice Thickness (H)(mm)	4
Stiffener Orientation (θ)	28.2

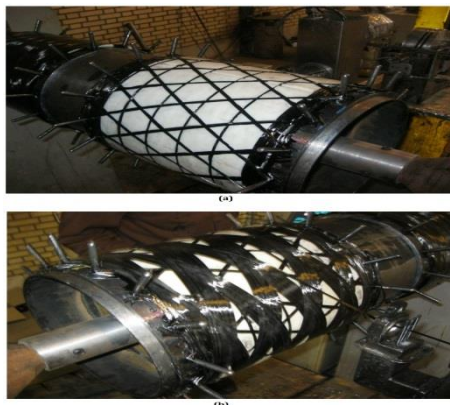


Figure 3. Fabrication process of the specimens using the filament winding method: (a) lattice winding, (b) shell winding.



Figure 4. The specimen under the experimental test.

4. Results

In this study, two types of specimens were considered. The experimental results were compared with a numerical (FEM) solution. Figure 5 shows a comparison between the experimental and numerical procedures for the specimen without skin. The experimental and numerical results obtained for the buckling test of the samples with the outer skin are shown in Figure 6.

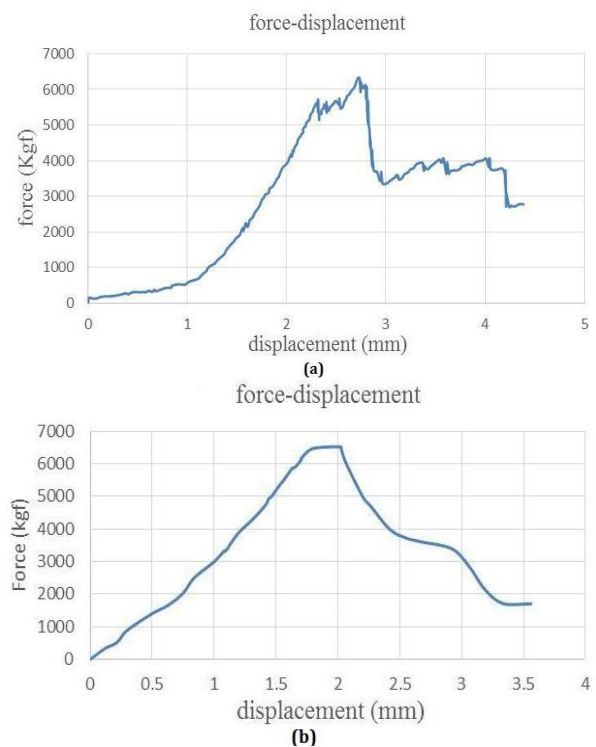


Figure 4. Buckling loads versus displacement for the specimen without an external skin: (a) experimental results, (b) numerical results.

Comparing the results displayed in Figures 5 and 6, the skin had a tremendously positive effect on increasing the buckling strength of the lattice structures. The buckling strength of the specimen with the outer skin was about 12.2 tonf, while the same measurement for the structure without the skin was about 6.3 tonf. The weight added to the structure by the skin was about 0.3 kg, while the buckling strength nearly doubled. In addition, Figures 5 and 6 show that the numerical results have good agreement with the experimental results. Figures 7 and 8 show the specimens after the buckling test in both numerical and experimental procedures.

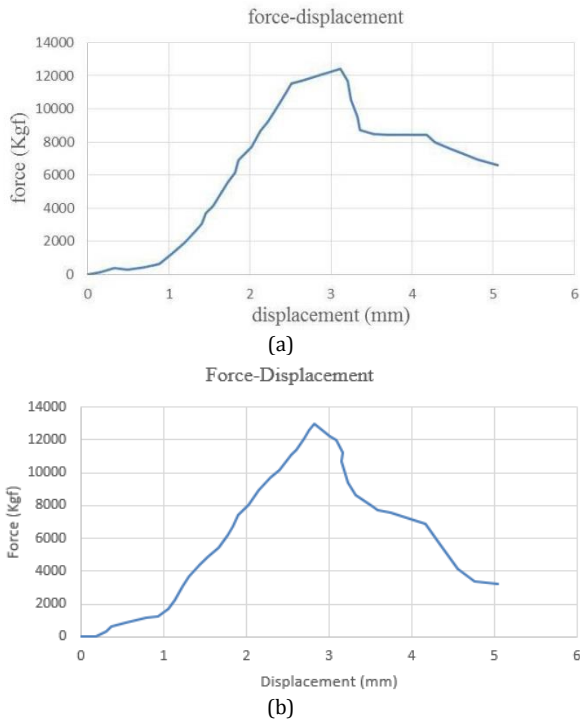


Figure 5. Buckling loads versus displacement for the specimen with an external skin: (a) experimental results, (b) FEM analysis.

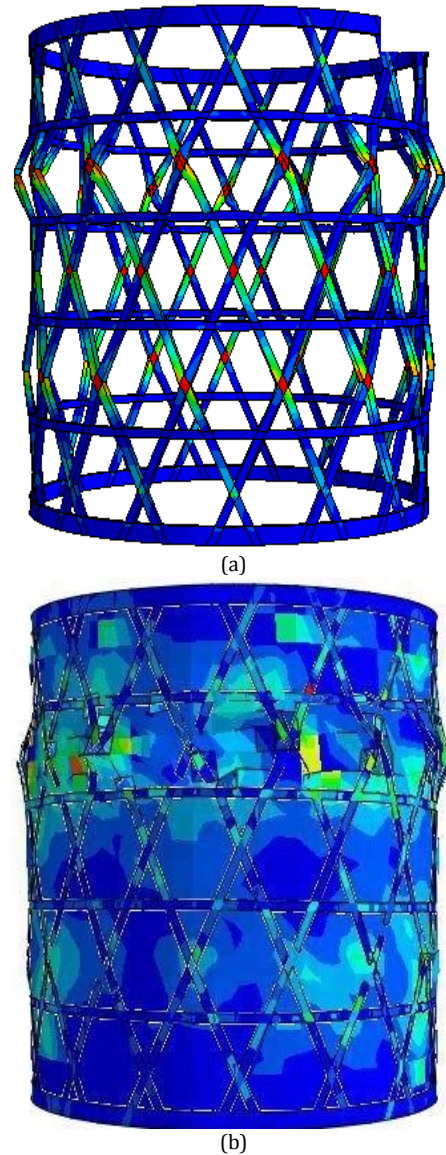


Figure 6. FEM analysis: (a) specimen without skin, (b) specimen with skin.

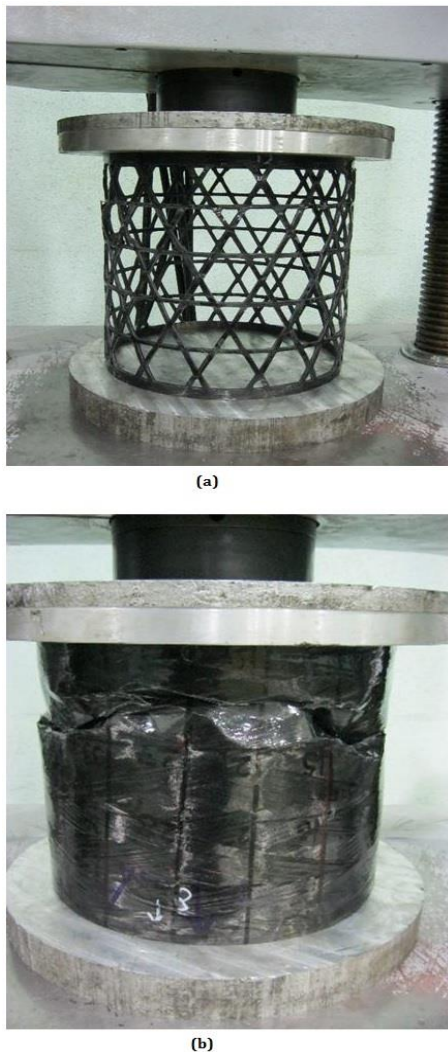


Figure 7. The specimens post-testing: (a) specimen without skin, (b) specimen with skin.

5. Conclusion

In this paper, the effect of an outer skin on the buckling strength of composite lattice cylinders was studied. By using the filament winding process, two types of specimens were fabricated: one with and one without an outer skin. Numerical and experimental analyses were carried out on the manufactured samples. The buckling strength of the structure with external skin was much enhanced over the strength of the structure without the external skin. The skin supports the stiffeners in a way that the skin increased the buckling strength significantly. Since the weight of the skin is negligible, when compared to the weight of the overall structure, the addition of the skin to the structure increased the buckling strength to weight ratio exponentially. Finally, the numerical and experimental results showed good agreement with one another.

References

- [1] Kidane S, Li G, Helms J and et al. Buckling load analysis of grid stiffened composite cylinders, *Compos Part B* 2003; 34: 1-9.
- [2] Ghasemi MA, Yazdani M, Hoseini SM. Analysis of effective parameters on the buckling of grid stiffened composite shells based on first order shear deformation theory. *Modares Mech Eng J* 2013; 13(10): 51-61.
- [3] Khalili SMR, Azarafza R, Davar A. Transient dynamic response of initially stressed composite circular cylindrical shells under radial impulse load. *Compos Struct* 2009; 89: 275-284.
- [4] Arashmehar J, Rahimi GH, Rasouli SF. Numerical and experimental stress analysis of stiffened cylindrical composite shell under transverse end load, *World Acad Sci Eng Technol* 2012; 6: 07-22.
- [5] Ghasemi MA, Yazdani M, Soltan Abadi E, Buckling behavior investigation of grid stiffened composite conical shells under axial loading, *Modares Mech Eng J* 2014; 14(15): 170-176.
- [6] Vasiliev VV, Barynin VA, Rasin AF. Anisogrid composite lattice structures – Development and aerospace applications, *Compos Struct* 2012; 94: 1117-1127.
- [7] Bisagni C, Cordisco P. Post-buckling and collapse experiments of stiffened composite cylindrical shells subjected to axial loading and torque, *Compos Struct* 2006; 73: 138-149.
- [8] Buragohain M, Velmurugan R. Buckling analysis of composite hexagonal lattice cylindrical shell using smeared stiffener model, *Defense Sci J* 2009; 59(3): 230-238.
- [9] Rahimi GH, Zandi M, Rasouli SF. Analysis of the effect of stiffener profile on buckling strength in composite isogrid stiffened shell under axial loading, *Aerosp Sci Technol* 2013; 24: 198-203.
- [10] Huang L, Sheikh AH, Ng C and et al. An efficient finite element model for buckling analysis of grid stiffened laminated composite plates, *Compos Struct* 2015; 122: 41-50.
- [11] Sun J, Lim CW, Xu X and et al. Accurate buckling solutions of grid-stiffened functionally graded cylindrical shells under compressive and thermal loads, *Compos Part B* 2016; 89: 96-107.